



Open Archive Toulouse Archive Ouverte

OATAO is an open access repository that collects the work of Toulouse researchers and makes it freely available over the web where possible

This is an author's version published in: <https://oatao.univ-toulouse.fr/26049>

Official URL :

<https://doi.org/10.1016/j.seppur.2019.115920>

To cite this version:

Lan, Yandi and Barthe, Laurie and Azaïs, Antonin and Causserand, Christel *Feasibility of a heterogeneous Fenton membrane reactor containing a Fe-ZSM5 catalyst for pharmaceuticals degradation: Membrane fouling control and long-term stability*. (2019) Separation and Purification Technology, 231. 115920. ISSN 1383-5866

Any correspondence concerning this service should be sent to the repository administrator: tech-oatao@listes-diff.inp-toulouse.fr

Feasibility of a heterogeneous Fenton membrane reactor containing a Fe-ZSM5 catalyst for pharmaceuticals degradation: Membrane fouling control and long-term stability

Yandi Lan, Laurie Barthe, Antonin Azais, Christel Causserand*

Laboratoire de Génie Chimique, Université de Toulouse, CNRS, INPT, UPS, Toulouse, France

ARTICLE INFO

Keywords:

Microfiltration
Membrane ageing
Slurry catalyst
Water treatment

ABSTRACT

Fenton oxidation is one of the promising advanced oxidation processes for the efficient elimination of pharmaceuticals from wastewater. The strong oxidation ability of this process is attributed to the generation of highly reactive hydroxyl radicals ($\cdot\text{OH}$) in the solution. In the present study, heterogeneous micro-sized zeolite catalysts that contain iron have been used in the Fenton-like process. This process enables operation in a wide pH range and facilitates the reuse of catalysts. Indeed, the coupling of the heterogeneous Fenton reaction with membrane filtration will ensure catalyst retention in the effluent compartment during the continuous water treatment. This study then investigated the fouling control strategies and membrane long-term stability in the heterogeneous Fenton reactor. During the filtration of the zeolite catalyst suspension, the critical flux for irreversible fouling was determined. One of the strategies to control membrane fouling can then be to choose an operating flux below this critical flux. In the case where a flux value above the critical flux is chosen, the results demonstrated total efficiency of hydrodynamic backwashing to eliminate hydraulically reversible fouling. Concerning the question of polymeric membrane long-term stability, it has been demonstrated that due to contact with the Fenton medium, membrane material undergoes oxidation and polymeric chain scissions. This latter is strongly linked to the decline in the mechanical resistance of membranes. In the tested conditions, despite the degradation to membrane material, the critical flux for irreversible fouling remained unchanged on aged membranes.

1. Introduction

The widespread presence of micropollutants in aquatic environments emerges as a sensitive issue [1–3]. Since most pharmaceuticals are only partially biodegradable, or even resistant to the conventional activated sludge process of a wastewater treatment plant (WWTP), refractory pharmaceuticals from all kinds of wastewater are released into the environment [4,5]. The accumulation of pharmaceuticals in the aquatic ecosystems poses significant threats to the ecosystem's sustainability and drinking-water safety [6,7]. As the use of pharmaceuticals dramatically increases, it is becoming increasingly important to develop and apply more efficient water treatment technologies for the removal of refractory pharmaceuticals from effluents.

Advanced oxidation processes (AOPs) are proving to be a promising alternative to traditional wastewater treatment techniques. AOPs generate a sufficient quantity of highly reactive oxidant species, such as hydroxyl radicals ($\cdot\text{OH}$) and sulphate radicals ($\text{SO}_4^{\cdot-}$) which allow the degradation of a large range of refractory organic compounds. Among

the AOPs, Fenton oxidation involves hydrogen peroxide as the oxidant and ferrous ions as catalysts to generate $\cdot\text{OH}$. Hydroxyl radicals are powerful oxidants with a high oxidation potential (2.8 eV). Fenton oxidation has been extensively studied for several decades and is recommended for the elimination of refractory pharmaceuticals [8,9]. Nevertheless, in a traditional Fenton process, the narrow operative pH window (2–4) limits its application. In addition, the presence of dissolved ferrous ions in the solution requires a post treatment before discharging the final effluents. To overcome these drawbacks, heterogeneous catalysts have been used in the Fenton-like process. This process enables operation in a wide pH range and facilitates the reuse of catalysts [10]. Heterogeneous Fenton-like catalysts contain iron solids. In addition to the use of solid iron-oxide minerals or zero-valent iron, a wide range of solid supports, such as zeolites, activated carbon or mesoporous materials are applied [11]. Zeolites have been extensively studied as Fenton-like catalyst supports for the oxidation of pollutants in wastewater [12–15].

Furthermore, the coupling of the heterogeneous Fenton reaction with

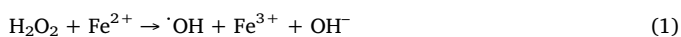
* Corresponding author at: Laboratoire de Génie Chimique, Université Paul Sabatier, 31062 Toulouse Cedex 9, France.

E-mail address: caussera@chimie.ups-tlse.fr (C. Causserand).

membrane filtration ensures that the catalyst is reused in the reactor. Hollow-fibre membranes are increasingly used in water treatment industry, as they exhibit more surface area per unit volume than flat sheet membranes. They are also flexible for applications at various scales [16]. Therefore, the development of a heterogeneous Fenton membrane reactor using hollow-fibre membranes is of great interest. An immersed retention system contributes furthermore to lower energetic consumption compared to an external tangential filtration (e.g. immersed membrane < 0.5 kWhm⁻³; external filtration module > 1 kWhm⁻³) in addition to being a compact system. Nevertheless, various fouling phenomena involving a cake layer formation or membrane structure and internal pores blockage have been reported when membranes are used for separating the catalysts from the reactive medium in Fenton or photo catalysis systems [17–19]. The catalyst particles in the heterogeneous Fenton membrane reactor potentially accumulate on the membrane surface under the driving force (transmembrane pressure) and lead to membrane fouling. Regarding the reversibility of fouling, membrane fouling can be characterized as either reversible or irreversible. A reversible accumulation of foulants will be partially or totally released from the membrane surface when transmembrane pressure decreases. An irreversible accumulation of foulants will remain on the membrane even if the driving force has stopped. Moreover, irreversible fouling could result in a dramatic decrease in flux (constant pressure filtration mode) or an increase in transmembrane pressure (constant permeate flux mode), leading to a decline in the process productivity and membrane lifetime. Therefore, the mitigation of irreversible fouling is of significant interest to the long-term sustainability of heterogeneous Fenton oxidation systems coupled to membrane filtration. Previous studies found that irreversible fouling may be prevented by operating below the critical flux for irreversibility during the filtration [20,21]. The critical flux for irreversibility is defined as the permeate flux below which a decline of flux over time (due to irreversible fouling) does not occur; above critical flux irreversible fouling is observed [20]. Operating the system below the critical flux for irreversibility can be an interesting strategy for controlling the irreversible fouling by catalysts in the heterogeneous Fenton membrane reactor. Additionally, when filtration conditions in a hollow-fibre membrane system lead to irreversible fouling, hydrodynamic backwashing can be an efficient procedure to remove this fouling layer. Fouling will be considered in this case as hydraulically reversible. Nevertheless, the efficient removal of fouling by backwashing depends on both the foulants and the fouling types [22].

Moreover, the long-term efficiency of the heterogeneous Fenton oxidation systems coupled to membrane filtration requires investigation on membrane stability in the heterogeneous Fenton reactive solution. Membrane ageing has been observed when polymeric membranes are exposed to oxidative chlorine solution used for membrane chemical cleaning [23–25]. Oxidants, such as sodium hypochlorite, react with membrane material, leading to a chemical change in membrane structure (membrane degradation). Degradation causes detrimental effects on membrane performances, including loss of selectivity, and shortens membrane lifetime by decreasing the membranes' mechanical strength. Previous studies indicate that ·OH radicals present in sodium hypochlorite oxidative solution play an important role in membrane ageing [23].

It is generally accepted that the traditional homogeneous Fenton reaction follows a free radical mechanism [26]. Two types of oxidants are present in the homogeneous Fenton reactive solution: H₂O₂ and radicals, mainly ·OH that are produced by the Fenton reaction (Eq. (1)) in the presence of catalysts.



The mechanisms producing hydroxyl radicals in the heterogeneous Fenton-like reaction using Fe-loaded zeolites has been less investigated than those involved in bleach solution and homogeneous Fenton. Two possible mechanisms can be proposed: a heterogeneous Fenton reaction mechanism induced by iron surface species on the zeolite and a

homogeneous Fenton reaction mechanism induced by leached iron in the solution [27]. So, the molecules within the solution may either be oxidized by the reactive species (that are generated by the iron leached into the solution), or oxidized by the iron species (that are located at the external surface of zeolites) [28]. Concerning membrane degradation by oxidants in the reactive medium, we could expect less degradation of membrane material in the heterogeneous Fenton suspension than in bleach or in homogeneous Fenton solution. This is expected if, on one hand, iron leaching is negligible and/or, on the other hand, the physical contact between catalysts and the membrane is reduced, scilicet in the case of low catalysts fouling. To elucidate this point, membrane ageing phenomena in a heterogeneous Fenton system requires specific investigation.

Few studies considered membrane coupling with heterogeneous Fenton reactors. Zhang et al. [17] investigated a heterogeneous Fenton-like membrane reactor using Y-shape zeolite slurry catalysts. In their study, the degradation efficiency of target organic dye, acid orange II, reached 97% in the reactor with an operating flux below a critical flux, this latter being estimated by the stepwise flux increase method. The durability of membranes was discussed through the monitoring of membrane flux vs. soaking time in the Fenton-like solution. In these tests, the authors underlined some inconsistent observations between no noticeable change in flux and a decrease in membrane weight. This latter can be attributed to membrane oxidation.

The present work exploits the heterogeneous Fenton hollow-fibre membrane (HFHFM) reactor for the degradation of pharmaceuticals from water. The objective of this study is to progress in membrane fouling management and in long-term stability analysis in a heterogeneous Fenton-like suspension. Considering their high catalytic activity and their good recycling capacity, the micro-sized Fe-zeolite catalyst, Fe-ZSM5, was used. Hollow-fibre membranes were immersed into the heterogeneous Fenton reactor for retention and reuse of this zeolite catalyst. Polysulfone (PSU) hollow-fibre membranes were tested as they are widely used in water treatment application. Ibuprofen was chosen as the targeted pharmaceutical to test the oxidative performances of the HFHFM reactor. This was the selected pharmaceutical because it is consumed in large quantities; its conjugates exhibit high acute toxicity and, whilst it is known to be biodegradable, it has been detected in wastewater treatment plant effluents and in surface water [29,30]. In order to acquire information necessary for the control of membrane fouling, firstly, the critical flux for irreversibility was determined in the HFHFM reactor. This was done according to the square wave method which was initially used to determine critical flux for irreversibility in model colloidal suspension [31], and recently in wastewater [21]. The square wave method allows for the distinction between the reversible and irreversible portions of fouling when a flux reduction is observed. This method detects the accurate value of irreversible fouling resistance for a range of permeate fluxes. Secondly, concerning the filtration conditions for which irreversible fouling occurs in the HFHFM reactor, the effectiveness of hydrodynamic backwashing was studied. This part of the work allowed the evaluation of the hydraulic reversibility of the ZSM5 zeolite deposit.

The following step was to analyse membrane stability in the heterogeneous Fenton medium. The Fe-ZSM5 catalyst exhibits very low leaching (corresponding to 0.03% of the total iron content in catalysts) and the activity of the leached iron in solution is negligible [15]. Due to this, we expected the oxidation of membranes by the reactive species present very close to the catalyst surface. In order to evaluate if the filtration process causes additional effects on membrane stability in Fenton medium, the membrane stability was determined in both static and filtration conditions. In the first case, membranes were soaked in an ageing solution, containing H₂O₂ and a catalyst, to mimic reactive medium. The membrane samples were collected over time and characterized using several techniques allowing different levels of analysis, from a molecular to a microscopic scale. Water permeability, mechanical properties and chemical structure (FTIR, EDX) of the membranes

were monitored. In filtration conditions, filtration-backwashing cycles were performed. The physical and chemical properties of membranes in the HFHFM reactor were analysed after 12-day cycles and compared with those in static conditions (soaking). The effect of exposure to a Fenton reactive solution during these filtration-backwashing cycles on critical flux for irreversible fouling was investigated. It revealed stability of membrane performance at a macroscopic level.

2. Experimental

2.1. Chemicals and membrane

All aqueous solutions were prepared using deionized water generated by a PURELAB maxima system (ELGA labwater's, UK). Ibuprofen (IBP, $C_{13}H_{18}O_2$, purity 99.99%) was purchased from BASF Corporation and used as received. Hydrogen peroxide (H_2O_2 , 30% w/w), sulphuric acid (1 mol/L), titanium tetrachloride solution (0.09 M in 20% HCl) for H_2O_2 concentration analysis, monopotassium phosphate (KH_2PO_4) and sodium phosphate dibasic dehydrate ($Na_2HPO_4 \cdot 2H_2O$) for preparing the buffer solution were purchased from Sigma-Aldrich. A commercial iron-containing zeolite of ZSM-5 structure (provided by Clariant™) was used as Fenton's reagents. This zeolite exhibited a Si/Al ratio of 13 and an iron content of 3.5 wt%. The average particle size of this catalyst is around 8 μm [15].

MF0808XS Polysulfone/Polyvinylpyrrolidone (PSU/PVP, molecular structures presented in Fig. 1) hollow-fibre membranes module (provided by Polymem™) was tested. PVP is blended (5%, w/w) into the PSU matrix to increase the hydrophilicity of the membranes.

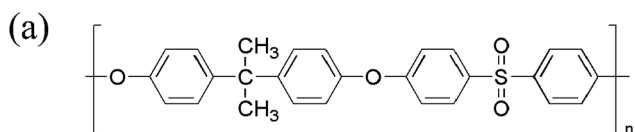
Each module contains 200 fibres with a pore size of 0.1 μm (microfiltration membrane). Its total active membrane surface is around 0.07 m^2 . Firstly, the module was used for testing the fouling control strategies and the efficiency of the hybrid oxidation process. Secondly, the long-term stability of the membranes was studied.

2.2. Experimental set-up and protocol

2.2.1. Heterogeneous Fenton hollow-fibre membrane reactor set-up

The heterogeneous Fenton hollow-fibre membrane reactor set-up is shown in Fig. 2. The experimental solution was introduced in a 6.5 L thermo-regulated glass reactor. A membrane module was immersed in the reactive solution to retain the catalyst in the glass reactor. Purified water was obtained through the membrane on the permeate side. The filtrations were performed in the outside-in filtration mode. Filtration fluxes were set by selecting the corresponding pump rotation, and the variation of both the flux and the transmembrane pressure was monitored over time. The rotation rate of the stirrer inside the reactor was 300 rpm during filtration. In this preliminary study, the permeate was recycled back into the reactor to simulate a continuous process from a hydrodynamic point of view.

The oxidation of pharmaceuticals in the HFHFM reactor was performed for the degradation of ibuprofen (IBP) in a synthetic solution, which was prepared by dissolving IBP under stirring for 10 h in distilled water. The initial concentration of IBP was 20 mg/L in this preliminary study, in order to achieve sufficient analytical precision from HPLC measurements. The stoichiometric amount of H_2O_2 (6.4 mM) was applied twice to avoid extensive scavenging of hydroxyl radicals. For effective production of hydroxyl radicals, the $[H_2O_2]/[Fe]$ molar ratio was maintained at 10, and the catalyst concentration at 4.8 g/L. This concentration corresponds to 0.62 mM of accessible iron, according to



iron dispersion measured by CO chemisorption. In this Fe-loaded ZSM5 zeolite catalyst suspension with the chosen operating conditions (H_2O_2 concentration of 6.4 mM at 25 °C), iron leaching is very low. The dissolved concentration of iron in the solution is approximately 0.048 mg/L. This value is too low to consider a possible IBP oxidation [15].

The Oxidation experiment was conducted at a controlled temperature of 25 ± 2 °C. The IBP solution and catalyst were added to the glass reactor over a period of 2 h whilst stirring and maintaining a controlled temperature, in order to reach a steady state in terms of adsorption of IBP on the catalyst. After, the suspension was circulated in the filtration system until the IBP concentration was constant (for a duration of 180 min). This was done to see whether the IBP adsorbed onto the membrane structure. After this, oxidation was started by adding H_2O_2 . The H_2O_2 concentration was maintained at 6.4 mM thanks to its continuous injection using a syringe pump (Harvard PHD 2000) during oxidation. During the experiments, solution samples were taken at regular intervals in the reactor. A previous study showed that the IBP concentration was stable and no degradation occurred in the sample solution after the removal of ZMS5 catalysts by filtration at an operating condition of 6.4 mM H_2O_2 , for pH 4 and for 6 h experimental time [15]. The samples were immediately treated by phosphate buffer (mixture of KH_2PO_4 0.05 M and $Na_2HPO_4 \cdot 2H_2O$ 0.05 M) to reach a neutral pH after the removal of catalysts by a 0.45 μm RC syringe filter for stopping the reaction.

2.2.2. Critical flux for irreversible fouling determination

The square-wave method, developed by Espinasse et al. [31], enables the hydraulic resistance to be distinguished. This resistance is induced by reversible (R_{rf}) and irreversible fouling (R_{if}). Reversible fouling is defined as that attributed to polarization concentration. This type of fouling disappears when the transmembrane pressure is stopped or decreased, whereas irreversible fouling is defined as the hydraulic resistance due to deposition or cake formation. By using the square-wave method, the accurate value of the critical flux for irreversible fouling (J_c) is obtained. When the filtration is operated for a flux above J_c , irreversible fouling takes place on the membrane surface. Different from the initial method in which the transmembrane pressure (TMP, referred to as ΔP in figures and equations) is controlled and the resulting permeate flux is monitored, the procedure used in the present study consists in altering the permeate flux with positive and negative variations, and in monitoring the resulting TMP as shown in Fig. 3.

The fluxes selected for the present study were 19, 21, 23, 25, 28, 32, 44 and 62 $L h^{-1} m^{-2}$. The values without asterisks correspond to upper flux steps while the asterisked ones correspond to lower flux steps. By comparing the measured transmembrane pressure between the steps that correspond to the same flux value/step, for example 21 and 21* $L h^{-1} m^{-2}$, the increase in TMP is associated to the fouling phenomenon that occurs at step 23 $L h^{-1} m^{-2}$. If the TMP is the same for steps 21 and 21* $L h^{-1} m^{-2}$, the fouling is considered as totally reversible and the flux (23 $L h^{-1} m^{-2}$) is below the critical value for irreversibility. If the TMP is not the same for steps 21 and 21* $L h^{-1} m^{-2}$, the fouling is partly irreversible and the flux (23 $L h^{-1} m^{-2}$) is above the critical value. Calculation methods of irreversible fouling are based on the relationship between the permeate flux and the fouling resistance:

$$J = \frac{\Delta P}{\mu_p (R_m + R_{if} + R_{rf})} = \frac{\Delta P}{\mu_p (R_m + R_f)} \quad (2)$$

where J is the permeate flux, ΔP is the transmembrane pressure, μ_p is

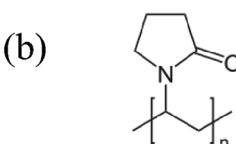


Fig. 1. Molecular structures of (a) PSU, (b) PVP.

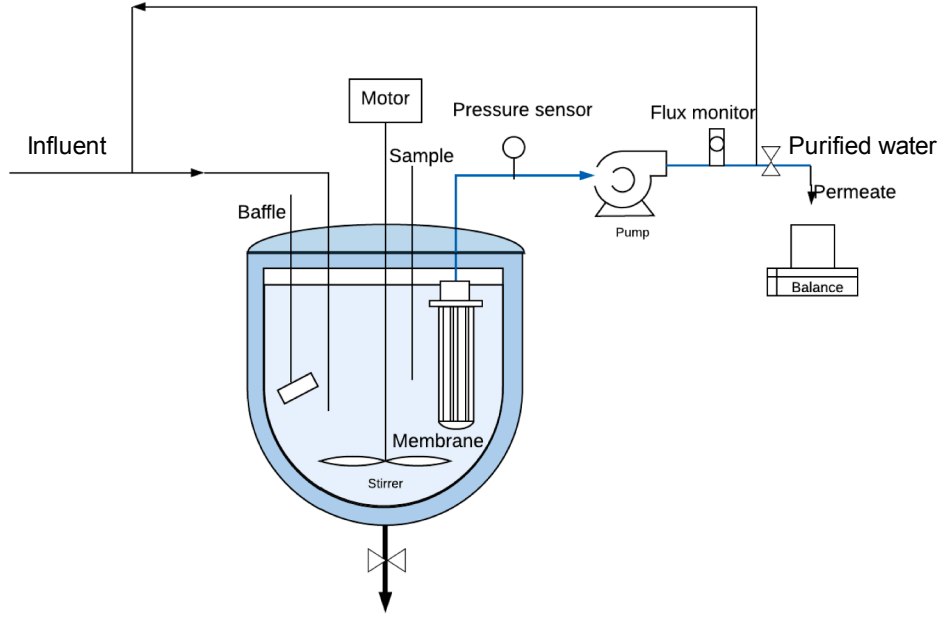


Fig. 2. Heterogeneous Fenton hollow-fibre membrane reactor set-up.

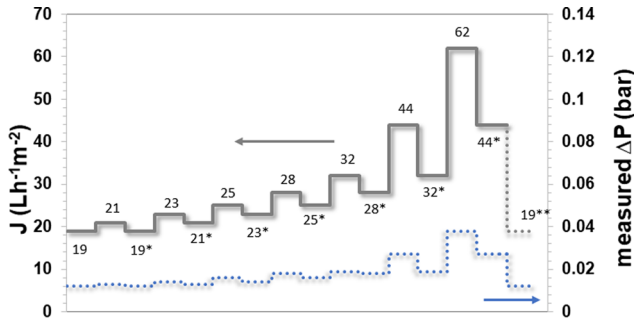


Fig. 3. Principle of the square-wave procedure; permeate flux vs. time; upper and lower steps. The continuous line represents the applied permeate flux; the dotted line represents the resulting transmembrane pressure.

the viscosity of the permeate, R_m is the intrinsic hydraulic membrane resistance, R_{if} the resistance due to the irreversible fouling, R_{rf} the resistance due to the reversible fouling (which is related to the polarization concentration) and R_f the total fouling resistance.

According to the square-wave filtration method, the irreversible fouling resistance that appears at upper flux steps (e.g. $23 \text{ L h}^{-1} \text{ m}^{-2}$) can be reached by comparing the fouling resistance at steps 21 and $21^* \text{ L h}^{-1} \text{ m}^{-2}$ as follows:

$$r_{if,23} = R_{f,21^*} - R_{f,21} \quad (3)$$

where $r_{if,23}$ is the irreversible fouling resistance relative to the step at $23 \text{ L h}^{-1} \text{ m}^{-2}$.

The value of the total R_{if} , at a given flux step is the sum of r_{if} at each previous pressure step.

$$R_{if} = \sum_n r_{if,n} \quad (4)$$

For example, $R_{if,23} = r_{if,21} + r_{if,23}$

In the present study, the filtration flux was either increased or decreased when the TMP change over a one-hour period was less than 2% of the initial value (accumulation of foulants reached a steady state). The irreversible fouling resistance was calculated for each flux step.

Membrane backwashing was applied when irreversible fouling occurred after the procedure of critical flux determination. For this purpose, the centrifugal pump was rotated in the reverse direction for 60 s

and the permeate (almost pure water) was pumped through the membrane back to the feed compartment under a flux equal to $19 \text{ L h}^{-1} \text{ m}^{-2}$ in our experiment.

2.2.3. Long-term membrane stability test

Long-term membrane stability in the Fenton membrane reactor was tested by soaking PSU/PVP membrane fibres in a heterogeneous Fenton reactive medium at a Fenton membrane reactor concentration. All soaking experiments were performed at a controlled temperature $25 \pm 2 \text{ }^\circ\text{C}$, maintained by a thermostatic bath and under stirring with a magnetic stirrer. The PSU/PVP membrane fibres were totally immersed in the suspension containing 4.8 g L^{-1} of ZSM-5 zeolite catalyst in the absence (as reference) or in the presence of $6.4 \text{ mM H}_2\text{O}_2$. The H_2O_2 concentration in the soaking suspensions was maintained at 6.4 mM by continuous H_2O_2 injection using a syringe pump (Harvard PHD 2000).

In the Fenton reactive suspension, two kinds of oxidants can potentially degrade membranes: H_2O_2 and reactive species. These latter, among them we can mention $\cdot\text{OH}$, are produced by the heterogeneous Fenton-like reaction on or very close to the zeolite catalyst surface. In order to identify the role of these two oxidants on membrane ageing, other groups of PSU/PVP membranes were immersed into $6.4 \text{ mM H}_2\text{O}_2$ solution for comparison. The pH was adjusted to 4.3 in the catalyst suspension. The soakings were performed for 35 days and membrane samples were taken every 4 days for analysis.

2.3. Analytical methods

2.3.1. Solutions' analysis

The IBP concentration was measured by liquid phase chromatography with UV detection at $\lambda = 222 \text{ nm}$ (PDA detector, Thermo Finnigan). Separation was performed on a C18 reverse phase column (ProntoSIL C18 AQ $5 \mu\text{m}$, $250 \times 4 \text{ mm}$) maintained at $40 \text{ }^\circ\text{C}$. The mobile phase consisted in a mixture of acetonitrile and water. This latter was acidified with phosphoric acid at $0.1\% \text{ v/v}$ and was fed in isocratic mode (60/40) at 1 mL/min . Samples were readily injected in the chromatograph after buffer treatment and filtration. The injection volume was set to $20 \mu\text{L}$ and the detection limit of IBP was $10 \mu\text{g/L}$.

Residual concentration of H_2O_2 was determined by the titanium tetrachloride method [32].

2.3.2. Membrane characterization

2.3.2.1. Scanning electron microscope with energy dispersive X-ray spectroscopy (SEM-EDX). Morphology and elemental information on the membrane surface were examined with a SEM (Hitachi Table top Microscope TM-1000) interfaced with an EDX spectroscopy system (Thermo-Fisher). Samples were coated with a thin layer of gold before SEM analysis for better contrast. EDX analyses were carried out at the same time. EDX measurements were taken at different locations of the membrane surface in order to obtain a comprehensive elemental composition.

2.3.2.2. ATR-FTIR. The ATR-FTIR spectra (Attenuated Total Reflection – Fourier Transform InfraRed spectroscopy) were obtained with a Thermo-Nicolet Nexus 670 apparatus (USA). The sample was placed on diamond crystal substrates and the analytical depth was approximately 2 μm . Virgin and aged membrane samples were firstly dried at 40 °C for 48 h. They were examined using ATR-FTIR spectra to identify chemical membrane changes after soaking in reactive medium. All the PSU/PVP IR spectra recorded were corrected by adjusting the 1587 cm^{-1} band to an arbitrary chosen absorbance value of 1. This band corresponds to aromatic in-plane ring bend stretching vibration of PSU [33] and considered to be invariable during the membrane degradation. The corrected absorbance is mentioned as relative absorbance. To facilitate the reader's understanding, when monitoring changes of specific IR bands upon degradation, normalization back to the pristine membrane relative absorbance may be performed.

2.3.2.3. Tensile testing. Tensile tests were performed on wet membranes using an INSTRON 4281 series tensile apparatus. Tailor-made grips for the hollow-fibre geometry were fitted to the device to avoid stress concentration. Initial distance between grips was fixed to 50 mm and samples were extended at a constant elongation rate of 100 mm/min. Ultimate tensile stress and ultimate elongation at break point were calculated from the experimental stress-strain curves. A set of five samples were analysed and averaged for each tested condition.

2.3.2.4. Permeability measurements. Pure water permeability of membranes was quantified in the H FHFMR reactor at a controlled temperature of $25 \pm 5^\circ\text{C}$. Ultrapure water was forced to permeate from the outside to the inside of the membrane module before and after filtration-oxidation test. Transmembrane pressure was applied by adjusting a pressure valve at the retentate side. Pure water permeability (L_p/μ_p in $\text{L h}^{-1} \text{m}^{-2} \text{bar}^{-1}$) was then calculated from the following Darcy law:

$$J = \frac{L_p}{\mu_p} \Delta P \quad (5)$$

where J is the permeate flux ($\text{L h}^{-1} \text{m}^{-2}$), ΔP is transmembrane pressure (bar); L_p and μ_p are the permeability coefficient and water viscosity, respectively.

L_p/μ_p was then taken as the slope value of the linear relationship between ΔP and J values. For each measurement, five fluxes ranging from 10 to 100 $\text{L h}^{-1} \text{m}^{-2}$ were applied and the corresponding TMP was taken. The TMP resulted from the average of minimum three measurements. The experimental error on the permeability measurement was within $\pm 5\%$.

3. Results and discussion

3.1. Membrane fouling control

Membrane fouling control strategies in this study are twofold: (1) the optimization of permeate flux to be under critical flux in order to prevent irreversible fouling and, (2) the use of hydrodynamic backwashing, in case a higher flux is desirable and irreversible fouling

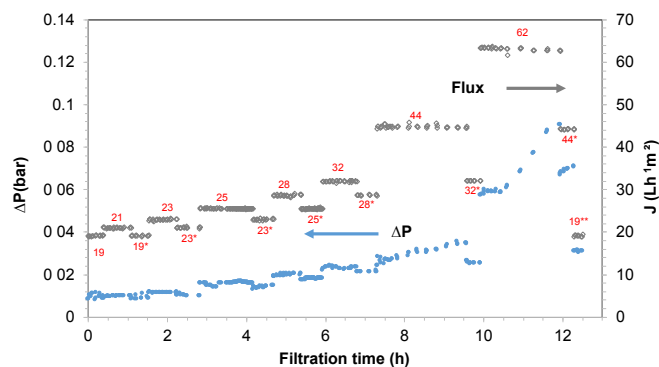


Fig. 4. Measured transmembrane pressure and imposed flux during the filtration of a 4.8 g/L catalyst suspension following the experimental procedure shown in Fig. 3.

occurs.

The critical flux for irreversibility was determined by the square-wave method following the experimental procedure shown in Fig. 3. The Zeolite catalyst suspension at 4.8 g L^{-1} was filtrated. The evolution of fluxes and transmembrane pressures are shown in Fig. 4. We can first observe that for the lower fluxes applied, for example 19 and $21 \text{ L h}^{-1} \text{m}^{-2}$, TMP did not increase over the duration of the step. Moreover, by comparing the value of TMP of two steps of the same flux value before and after $21 \text{ L h}^{-1} \text{m}^{-2}$ (respectively $19 \text{ L h}^{-1} \text{m}^{-2}$ and $19^* \text{ L h}^{-1} \text{m}^{-2}$), TMP was unchanged. This means that no irreversible fouling occurs at $21 \text{ L h}^{-1} \text{m}^{-2}$. In contrast, the stable TMP at the $44^* \text{ L h}^{-1} \text{m}^{-2}$ step is higher than the one at $44 \text{ L h}^{-1} \text{m}^{-2}$ step indicating that irreversible fouling occurs at $62 \text{ L h}^{-1} \text{m}^{-2}$. Therefore, the flux value of $62 \text{ L h}^{-1} \text{m}^{-2}$ is greater than the critical flux for irreversibility (J_c). After $44^* \text{ L h}^{-1} \text{m}^{-2}$ step, a decrease in flux to $19 \text{ L h}^{-1} \text{m}^{-2}$ was performed and presented as $19^{**} \text{ L h}^{-1} \text{m}^{-2}$ step. The fact that the stable TMP at the $19^{**} \text{ L h}^{-1} \text{m}^{-2}$ step is much higher than the value at $19 \text{ L h}^{-1} \text{m}^{-2}$ confirms that irreversible fouling occurs during the filtration.

Through the application of the square-wave method described in Section 2.2.2, the total irreversible fouling resistance at a given flux step and the value of the critical flux for irreversibility J_c were estimated. As shown in Fig. 5, the total irreversible fouling resistance at 19, 21, and $23 \text{ L h}^{-1} \text{m}^{-2}$ was negligible while it dramatically increased from 25 to $62 \text{ L h}^{-1} \text{m}^{-2}$ flux steps. The value of the critical flux for irreversibility was therefore estimated at $23 \text{ L h}^{-1} \text{m}^{-2}$. This means that irreversible fouling can be prevented by operating flux lower than this value during filtration of a 4.8 g L^{-1} zeolite catalyst suspension.

To reveal the effectiveness of reverse filtration in eliminating

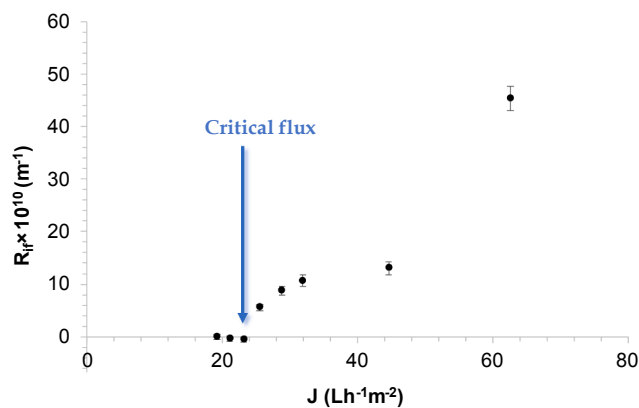


Fig. 5. Evolution of irreversible fouling resistance R_{if} vs. permeate flux during filtration of 4.8 g/L catalyst suspension and location of the critical flux for irreversibility.

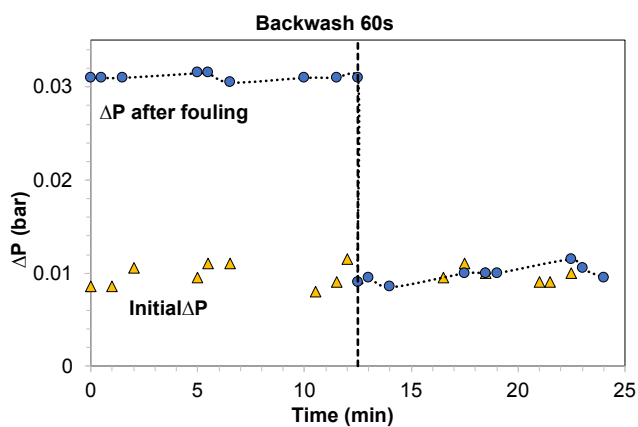


Fig. 6. Variation of transmembrane pressure vs time: ΔP at $19 \text{ L h}^{-1} \text{ m}^{-2}$ at initial step when no fouling occurs; ΔP at $19 \text{ L h}^{-1} \text{ m}^{-2}$ with fouling, before and after application of backwash.

fouling from the membrane surface in this system, we performed a backwash of the fouled membrane module after measuring the critical flux. For comparison, Fig. 6 plots the variation of transmembrane pressure initially measured at $19 \text{ L h}^{-1} \text{ m}^{-2}$ (triangle) and the TMP at the final step in Fig. 4 ($19 \text{ L h}^{-1} \text{ m}^{-2}$). This latter was monitored before and after application of a backwash (circle). A noticeable increase in transmembrane pressure is observed at the $19 \text{ L h}^{-1} \text{ m}^{-2}$ step due to the formation of irreversible fouling during the procedure. After the application of 60 s backwashing (under $19 \text{ L h}^{-1} \text{ m}^{-2}$ backwash flux) on this fouled membrane, one can observe that ΔP declined dramatically to reach its initial value when no fouling occurs. This result indicates that the backwash enables the removal of more than 99% of irreversible fouling in this system. It is worth noting that irreversible fouling described here is the portion attributed to catalyst deposition and cake formation, and remains when release of driving force. However, this irreversible fouling can be hydraulically reversible and removed by backwashing. This behaviour is consistent with fouling mainly due to cake formation on the membrane surface, considering a pore size of $0.1 \mu\text{m}$ vs. a catalyst particles' size of $8 \mu\text{m}$. This size ratio is in favour of total retention of particles that build a cake layer on the surface. This cake layer is easy to remove in most cases by backwash.

3.2. First evaluation of Fenton membrane reactor performances

In order to test the oxidation performance of the HFHFM reactor and verify the critical flux for irreversible fouling, the oxidation of IBP was performed at fluxes 20 and $30 \text{ L h}^{-1} \text{ m}^{-2}$, respectively below and above J_c ($23 \text{ L h}^{-1} \text{ m}^{-2}$). The suspension containing IBP and the catalyst was filtrated and recirculated in the reactor. When the concentration of IBP stabilized (180 min, the time required to reach an adsorption equilibrium of IBP on the membrane), H_2O_2 was injected and oxidation started. As shown in Fig. 7 (a), the removal rate of IBP is more than 99% after 180 min's oxidation in the reactor, regardless of the flux. Fig. 7 (b) shows the variation of transmembrane pressure vs. time. In the recirculation step, ΔP kept the same value over 180 min using $20 \text{ L h}^{-1} \text{ m}^{-2}$, confirming that no noticeable fouling occurs when the operating flux is below J_c . When the operating flux was $30 \text{ L h}^{-1} \text{ m}^{-2}$, an increase in ΔP of 45% in 180 min was observed, revealing that fouling occurs at a flux above J_c . After H_2O_2 injection, a non-expected slight increase of ΔP at $20 \text{ L h}^{-1} \text{ m}^{-2}$ was observed. When using $30 \text{ L h}^{-1} \text{ m}^{-2}$ the increasing rate of ΔP is greater (3.9 times more) than before the addition of H_2O_2 addition.

To try to understand this phenomenon, pure water permeability of the membrane module before and after oxidation (shown in Table 1) was compared. When the operation is performed at $20 \text{ L h}^{-1} \text{ m}^{-2}$, it can be found that pure water permeability of the membrane module

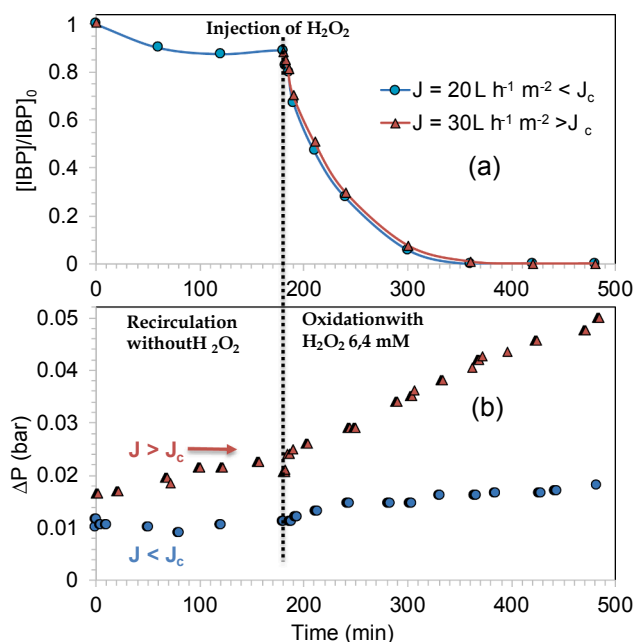


Fig. 7. Evolution of (a) IBP concentration and (b) transmembrane pressure during oxidation of IBP in the HFHFM reactor at two permeate fluxes: \bullet $20 \text{ L h}^{-1} \text{ m}^{-2}$ i.e. below the critical flux, \blacktriangle $30 \text{ L h}^{-1} \text{ m}^{-2}$ i.e. above the critical flux. $[\text{IBP}]_0 = 20 \text{ mg/L}$, $[\text{catalyst}] = 4.8 \text{ g L}^{-1}$, $[\text{H}_2\text{O}_2] = 6.4 \text{ mM}$, $\text{pH} = 4.3$.

Table 1

Pure water permeability of membrane (in $\text{L h}^{-1} \text{ m}^{-2} \text{ bar}^{-1}$) before and after oxidation at each flux.

	Permeability before oxidation	Permeability after oxidation
$J = 20 \text{ L h}^{-1} \text{ m}^{-2} < J_c$	$1658.8 \pm 5\%$	$1736.2 \pm 5\%$
$J = 30 \text{ L h}^{-1} \text{ m}^{-2} > J_c$	$1739.6 \pm 5\%$	$1455.7 \pm 5\%$

before and after oxidation was the same (if 5% experimental error is applied). This means no irreversible fouling and no change in membrane module seem to occur. In this case, the slight increase in ΔP after H_2O_2 injection may be related to the production of oxidation-generated bubbles. These bubbles may affect ΔP values or may cause other reversible changes in membrane. At $30 \text{ L h}^{-1} \text{ m}^{-2}$ water permeability decreased by 17%, validating the occurrence of irreversible fouling of the membrane module.

3.3. Long-term stability of membrane in heterogeneous Fenton medium

Long-term stability of PSU/PVP hollow-fibre membranes was studied after exposure to the heterogeneous Fenton medium. With that aim, membranes were soaked in a Fenton reactive medium (4.8 g L^{-1} catalyst and $6.4 \text{ mM H}_2\text{O}_2$) and in a simple catalyst suspension (4.8 g L^{-1} catalyst) that acts as reference. Changes in membrane performances and in chemical structure of membrane material were then monitored.

3.3.1. Effect of exposure to a Fenton reactive medium on membranes' mechanical properties and surface morphology

The effect of a heterogeneous Fenton reactive medium was first studied on a macroscopic scale with the monitoring of mechanical properties. These latter were evaluated by tensile testing. A typical shape of stress-strain curves obtained for pristine and Fenton medium soaked membrane samples is presented in Fig. S1 (supplementary information). The comparison of these curves shows that the shape of the elastic domain and early stages of the plastic domain are generally

unchanged, while the ultimate elongation value (at break) appears to be significantly affected. That is to say, during tensile testing, the membrane samples' break appeared sooner after exposure to Fenton medium than for virgin membrane. Therefore, the mechanical properties of the membrane are monitored by the changes of ultimate elongation as this was found to be the most sensitive parameter compared, for example, to Young's Modulus. The ultimate elongation measured was for pristine membranes: $110\% \pm 10\%$. For membranes after 35 days' exposure to a catalyst suspension (4.8 g L^{-1}): $114\% \pm 11\%$. Finally, for samples exposed 35 days to Fenton medium (4.8 g L^{-1} catalyst and $6.4 \text{ mM H}_2\text{O}_2$): $68\% \pm 27\%$. Considering the measurement errors in ultimate elongation, we observed, on one hand, that PSU/PVP membranes kept the same mechanical properties when soaked in a reference suspension (only a catalyst without oxidative agent). On the other hand, the ultimate elongation of membranes decreased by 40% after 35 days' exposure to the Fenton reactive medium.

Fig. S2 (supplementary information) presents the surface morphology of membrane samples after 35 days' exposure to a catalyst reference suspension and the Fenton reactive medium. Noticeable surface pitting and the disappearance of the regular pore structure in membrane samples exposed to Fenton medium was observed. These surface aspect changes are in accordance with results presented by several authors who also observed surface cracking and pitting of membranes after hypochlorite treatment [25,34,35].

3.3.2. Effect of exposure to Fenton reactive medium on membranes' chemical structure

As it has been found that prolonged contact with the Fenton reactive medium might induce a decline in membranes' mechanical properties and change to the surface morphology, this section is dedicated to investigating chemical reasons for these degradations.

The ATR-FTIR spectra of a pristine membrane and a PSU/PVP membrane after 35 days' exposure to the Fenton reactive medium were realized and reported in Fig. 8. The intensity of the IR band at 1674 cm^{-1} , corresponding to the stretching vibration of the amide unit of the PVP, decreased in the aged membrane in comparison to the pristine one. This indicates either a degradation of the PVP or a decrease in PVP content on the membrane. The degradation of PVP was confirmed by the appearance of bands at 1700 cm^{-1} and 1770 cm^{-1} . These bands indicate the formation of succinimide, a PVP oxidation product [36]. Pellegrin et al. observed similar variations of bands attributed to PVP degradation in hypochlorite treatment of PES/PVP membranes. The peak around 3350 cm^{-1} relating to phenol O-H stretching is probably linked to the formation of phenol on the PSU backbone. The absorbance band appearing at 1638 cm^{-1} could be associated to the formation of alkene groups by chain scissions of PSU

from the isopropylidene unit. Gaudichet-Maurin et al. found an IR absorbance peak at 1644 cm^{-1} during the characterisation of a PSU/PVP membrane aged in bleach solution. They suggested that the peak is related to the chain scission of isopropylidene bridges, probably resulting from hydrogen abstraction by a primary radical [24]. Rouaix et al [37] concluded that the evolution of the membrane structure shown by SEM is only due to PSU chain scission and not to the removal of PVP. This is because, after soaking in conditions for which removal of PVP is still effective but without degradation of PSU, no change in membrane morphology and no swelling were observed.

Fig. 9 shows the evolution of absorbance corresponding to the oxidation of (a) PVP and (b) PSU on PSU/PVP membranes against the number of soaking days. In Fig. 9(a), it can be clearly observed that, during the first few days, there is a decrease in the amide absorbance of the PVP (1674 cm^{-1}). After about 8 days' soaking, succinimide (1700 cm^{-1}) then starts to form. In Fig. 9(b), the oxidation of PSU is only observed after 14 days' exposure to the Fenton medium.

Considering the dramatic decrease in ultimate elongation of PSU/PVP membranes after exposure to the Fenton reactive medium, a link between this mechanical property change and the material chemistry modification was looked for. It was found that the ultimate elongation of PSU/PVP membranes is strongly related to the FTIR absorbance at 1638 cm^{-1} . This latter corresponds to the chain scission of PSU, as shown in Fig. 10. Therefore, the decrease in PSU/PVP membranes' mechanical property is closely correlated to the development of PSU chain scissions in the membrane material.

As mentioned in the introduction, two types of oxidants present in the Fenton reactive suspension are susceptible to degrade membranes: H_2O_2 and reactive species, such as $\cdot\text{OH}$. This latter is formed in the heterogeneous Fenton-like reaction on, or very close to, the zeolite catalyst surface. In order to identify the role of these two oxidants on membrane ageing, the chemical properties of the PSU/PVP membranes that were soaked in either a simple solution of H_2O_2 (pH adjusted to 4.3 by addition of $1 \text{ M H}_2\text{SO}_4$ so that it is the same as in the Fenton medium) or in the Fenton reactive medium, were compared. The FTIR spectra of PSU/PVP membranes soaked in H_2O_2 is shown in Fig. S3 (supplementary information). In this figure, the only modification, compared to the pristine membrane spectra, comes from the sharp decrease of the 1674 cm^{-1} band and the appearance of the 1700 cm^{-1} band, both related to PVP degradation. It has been therefore concluded that the oxidation and chain scissions of PSU in the Fenton medium results from the attack of reactive species formed in the heterogeneous Fenton-like reaction. EDX measurements were also conducted to investigate the modification of the chemical composition on H_2O_2 and on the membrane surface treated with the Fenton medium. Since PSU and PVP repeat units carry only one sulphur atom (S) and one nitrogen atom

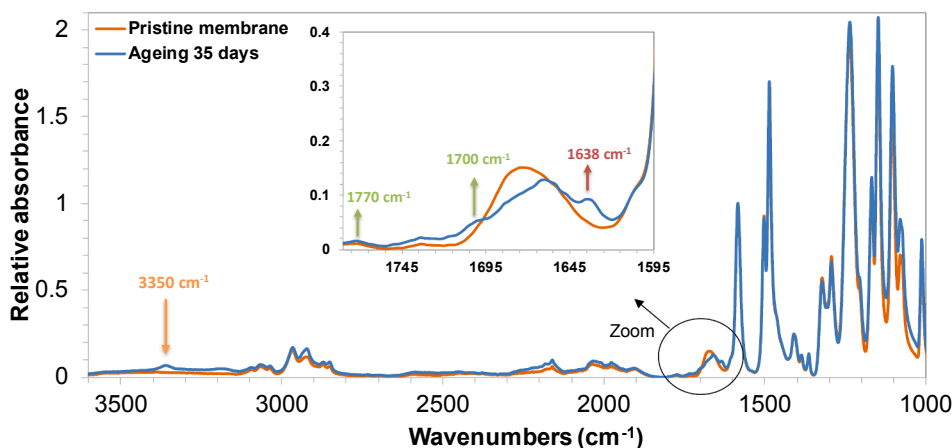


Fig. 8. ATR-FTIR spectra of a pristine membrane and a PSU/PVP membrane after 35 days' exposure to the Fenton reactive medium containing 4.8 g L^{-1} catalyst and $6.4 \text{ mM H}_2\text{O}_2$.

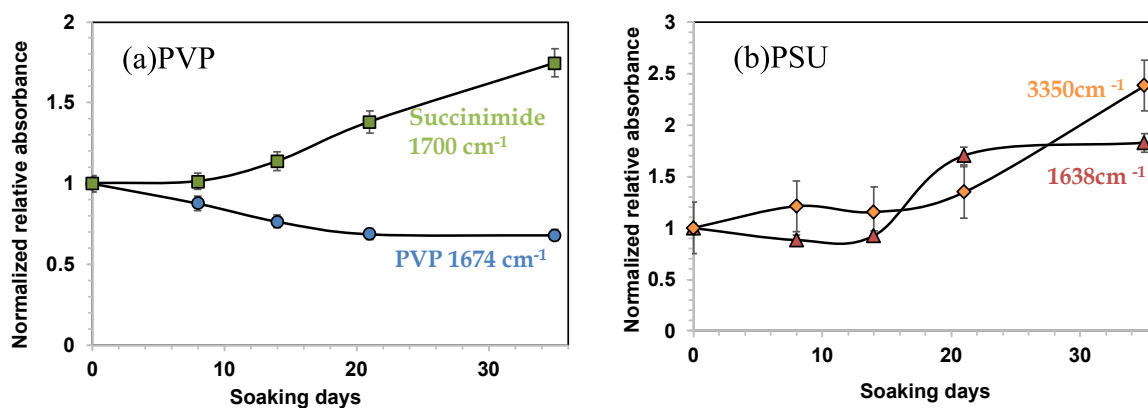


Fig. 9. Normalized relative FTIR absorbance corresponding to the oxidation of (a) PVP and (b) PSU on PSU/PVP membranes against number of soaking days in the Fenton reactive medium (4.8 g L^{-1} catalyst and $6.4 \text{ mM H}_2\text{O}_2$).

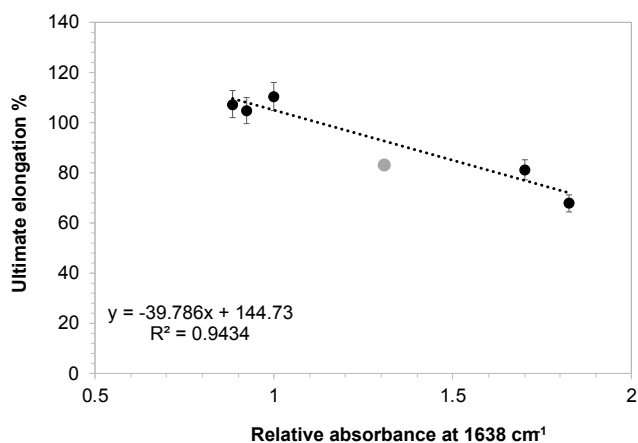


Fig. 10. Relationship between ultimate elongation of PSU/PVP membranes and FTIR relative absorbance at 1638 cm^{-1} (black symbol: contact by soaking; grey symbol: contact during filtration-backwashing cycles; see Section 3.3.3).

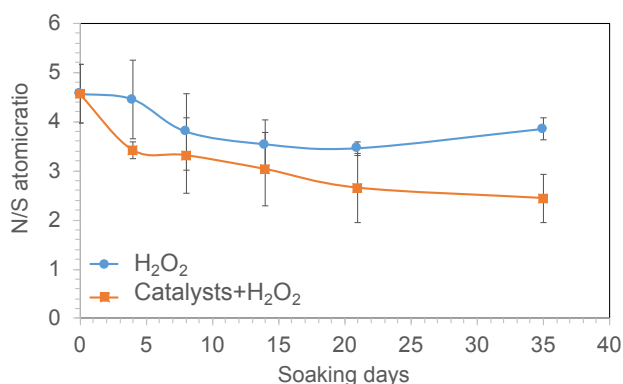


Fig. 11. Variation versus soaking time of N/S element percentage for membranes exposed to $6.4 \text{ mM H}_2\text{O}_2$ solution and to the Fenton reactive medium (4.8 g L^{-1} catalyst and $6.4 \text{ mM H}_2\text{O}_2$).

(N) respectively (Fig. 1), the N/S atomic ratio represents the evaluation of the fraction of PVP on the membrane surface. One can find that the N/S atomic ratio on samples' surface decreased after exposure to the two types of reactive medium (Fig. 11). Nevertheless, for the membranes exposed to H_2O_2 solution, the decline in N/S atomic ratio seems to occur only from 4 to 8 days and then reaches a plateau value. The total decrease being 15%. For membranes exposed to the Fenton reactive medium, the decline in N/S ratio lasts from the initial time to the end of the ageing test and the decrease reaches 47%. This result is in

accordance with FTIR measurements (Fig. 9 (a)). Obviously, membranes underwent more serious dislodgment of PVP when exposed to the Fenton reactive medium in which reactive species were formed.

Thus, it has been concluded that, in the heterogeneous Fenton reactive medium, reactive species formed in the heterogeneous Fenton-like reaction on, or very close to, the zeolite catalyst surface. These reactive species are the main cause of dislodgment of PVP from the membrane matrix and of the PSU chain scission. The main consequence on membrane performances of this material degradation is a decrease in PSU/PVP membrane mechanical resistance, which is likely to lead to the breaking of the hollow-fibre.

In the evaluation of the membrane lifetime in the HFHFM reactor, we should further consider that $\cdot\text{OH}$ radicals are generated onto the catalyst and will react next to the solid particles as their lifetime is very short (nanosecond). Therefore, a catalyst cake formation on a membrane surface during a filtration process could have adverse consequences on membrane ageing. The following paragraph will provide insights on this point.

3.3.3. Effect of exposure to Fenton reactive solution during filtration-backwashing cycles on critical flux for irreversible fouling

The aim of this last section was to compare critical fluxes for irreversibility measured on pristine and aged membranes. For this, in order to approximate the actual conditions of use, membranes immersed in the HFHFM reactor encountered several filtration – backwashing cycles corresponding to a cumulative exposure duration of 12 days to the Fenton medium. The permeate flux imposed during this experiment was $20 \text{ L h}^{-1} \text{ m}^{-2}$, that is to say lower than the critical flux measured on virgin membrane. Backwashing was nevertheless applied in order to help in keeping away catalyst particles from the membrane surface. The critical flux was then measured again, this time on the used module according to the procedure described in Section 2.2.2. At the end of these filtration cycles, membranes were sampled from the module, their chemical and mechanical characteristics were determined and the results were discussed in comparison to those obtained after soaking in the Fenton reactive medium (Section 3.3.2).

The properties of these aged membranes have been reported in Fig. 10 to identify the level of degradation reached by comparison to the ones qualified during soaking experiments. We can see that, after filtration cycles, the membranes simultaneously exhibited a decrease in ultimate elongation and an increase in relative absorbance at 1638 cm^{-1} , behaviour previously attributed to PSU chain scission. According to Figs. 9 and 10, the level of the degradation reached during these filtration-backwashing cycles (cumulative exposure duration of 12 days) corresponds to 14–20 days of soaking. From these results, the membrane ageing rate in the filtration system with intermittent accumulation of catalyst on membrane surface seems to be equivalent to the

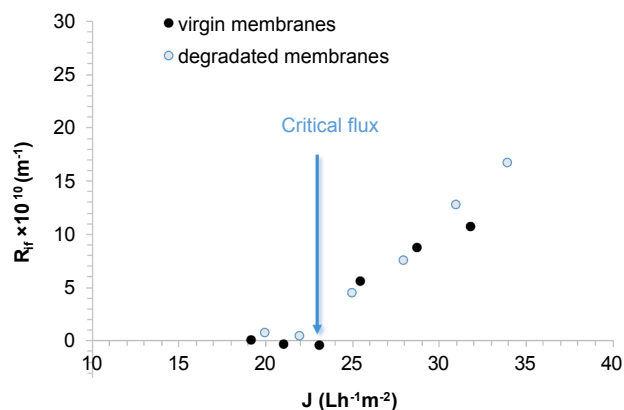


Fig. 12. Comparison of critical fluxes for irreversible fouling measured during filtration of a 4.8 g/L catalyst suspension on virgin hollow-fibres and on an aged membranes.

rate reached during simple soaking in the Fenton medium.

The comparison of critical fluxes for irreversibility measured on pristine and aged membranes is shown in Fig. 12. No noticeable change in the value of the critical flux was observed subsequent to membrane degradation after filtration cycles in the heterogeneous Fenton reactor. Changes in membrane structure and chemical properties obviously alter the hydrophilicity (degradation and departure of the hydrophilic additive PVP), surface roughness (Fig. S2), and catalyst particles-membrane material interactions. Despite all these changes, the membranes exhibit comparable behaviour at the macroscopic level towards fouling by particles during filtration. Moreover, no leak in particles was observed in the permeate during the filtration cycles.

4. Conclusion

This study investigated the fouling control strategies and the long-term stability of the PSU/PVP membrane in the HFHF membrane reactor. Firstly, the filtration of a zeolite catalyst suspension has enabled the critical flux for irreversible fouling to be determined. This value is approximately 23 L h⁻¹ m⁻². With the critical flux identified, one of the fouling control strategies is then to decide to select an operating flux below this critical flux. Secondly, in the case where a flux above the critical flux should be chosen for process productivity needs, our results demonstrated hydrodynamic backwashing to be efficient to eliminate irreversible fouling (mainly cake) in the tested conditions. In addition to other solutions, such as membrane shaking (not investigated in the present study), filtration-backwashing cycles are therefore an efficient procedure to remove Fe-ZSM5 catalyst deposition and to maintain membrane performance.

This study also investigated membrane stability in the heterogeneous Fenton system. Reactive species, such as ·OH radicals, heterogeneously distributed in the oxidative medium were identified as responsible for modifications to the chemical composition, the surface morphology and the mechanical properties of membranes. Due to contact with a Fenton medium, PVP oxidation and PSU chain scission occur, this latter being strongly linked to the decline in mechanical resistance of membranes (elongation at break decline of 40% after 35 days' exposure). In terms of PVP degradation and mechanical properties decline, concerning the membrane ageing rate, a similarity was observed between the soaking tests and during filtration-backwashing cycles at a flux lower than the critical flux. This result suggests that, in the conditions tested and for the same cumulative exposure duration, filtration of the catalyst suspension does not make the membrane degrade faster than in soaking conditions.

Despite these membrane material degradations, our experiments demonstrated no changes in the critical flux for irreversible fouling,

meaning that in the tested conditions the membrane fouling propensity is not affected by membrane ageing due to contact with the Fenton solution.

Acknowledgments

We are grateful for financial support from the ANR (French National Research Agency) via the "SOFENCoMEM" ANR project (ANR 14 CE04 0006).

Appendix A. Supplementary material

Supplementary data to this article can be found online at <https://doi.org/10.1016/j.seppur.2019.115920>.

References

- [1] D.W. Kolpin, E.T. Furlong, M.T. Meyer, E.M. Thurman, S.D. Zaugg, L.B. Barber, H.T. Buxton, Pharmaceuticals, Hormones and Other Organic Wastewater Contaminants in U.S. Streams, 1999–2000: A National Reconnaissance, *Environ. Sci. Technol.* 36 (2002) 1202–1211, <https://doi.org/10.1021/es011055j>.
- [2] K.S. Le Corre, C. Ort, D. Kateley, B. Allen, B.I. Escher, J. Keller, Consumption-based approach for assessing the contribution of hospitals towards the load of pharmaceutical residues in municipal wastewater, *Environ. Int.* 45 (2012) 99–111, <https://doi.org/10.1016/j.envint.2012.03.008>.
- [3] W.C. Li, Occurrence, sources, and fate of pharmaceuticals in aquatic environment and soil, *Environ. Pollut.* 187 (2014) 193–201, <https://doi.org/10.1016/j.envpol.2014.01.015>.
- [4] S. Rodríguez-Mozaz, S. Chamorro, E. Marti, B. Huerta, M. Gros, A. Sánchez-Melsió, C.M. Borrego, D. Barceló, J.L. Balcázar, Occurrence of antibiotics and antibiotic resistance genes in hospital and urban wastewaters and their impact on the receiving river, *Water Res.* 69 (2015) 234–242, <https://doi.org/10.1016/j.watres.2014.11.021>.
- [5] A.J. Watkinson, E.J. Murby, D.W. Kolpin, S.D. Costanzo, The occurrence of antibiotics in an urban watershed: From wastewater to drinking water, *Sci. Total Environ.* 407 (2009) 2711–2723, <https://doi.org/10.1016/j.scitotenv.2008.11.059>.
- [6] K. Kümmerer, Significance of antibiotics in the environment, *J. Antimicrob. Chemother.* 52 (2003) 5–7, <https://doi.org/10.1093/jac/dkg293>.
- [7] G.M. Bruce, R.C. Pleus, S.A. Snyder, Toxicological relevance of pharmaceuticals in drinking water, *Environ. Sci. Technol.* 44 (2010) 5619–5626, <https://doi.org/10.1021/es1004895>.
- [8] A.D. Bokare, W. Choi, Review of iron-free Fenton-like systems for activating H₂O₂ in advanced oxidation processes, *J. Hazard. Mater.* 275 (2014) 121–135, <https://doi.org/10.1016/j.jhazmat.2014.04.054>.
- [9] A. Babunussami, K. Muthukumar, A review on Fenton and improvements to the Fenton process for wastewater treatment, *J. Environ. Chem. Eng.* 2 (2014) 557–572, <https://doi.org/10.1016/j.jece.2013.10.011>.
- [10] A. Mirzaei, Z. Chen, F. Haghigat, L. Yerushalmi, Removal of pharmaceuticals from water by homo/heterogeneous Fenton-type processes – A review, *Chemosphere* 174 (2017) 665–688, <https://doi.org/10.1016/j.chemosphere.2017.02.019>.
- [11] P.V. Nidheesh, Heterogeneous Fenton catalysts for the abatement of organic pollutants from aqueous solution: a review, *RSC Adv.* 5 (2015) 40552–40577, <https://doi.org/10.1039/C5RA02023A>.
- [12] K. Fajrwergh, H. Debellefontaine, Wet oxidation of phenol by hydrogen peroxide using heterogeneous catalysis Fe-ZSM-5: a promising catalyst, *Appl. Catal. B Environ.* 10 (1996) L229–L235, [https://doi.org/10.1016/S0926-3373\(96\)00041-0](https://doi.org/10.1016/S0926-3373(96)00041-0).
- [13] E.V. Kuznetsova, E.N. Savinov, L.A. Vostrikova, V.N. Parmon, Heterogeneous catalysis in the Fenton-type system FeZSM-5/H₂O₂, *Appl. Catal. B Environ.* 51 (2004) 165–170, <https://doi.org/10.1016/j.apcatb.2004.03.002>.
- [14] A. Shahbazi, R. Gonzalez-Olmos, F.-D. Kopinke, P. Zarabadi-Poor, A. Georgi, Natural and synthetic zeolites in adsorption/oxidation processes to remove surfactant molecules from water, *Sep. Purif. Technol.* 127 (2014) 1–9, <https://doi.org/10.1016/j.seppur.2014.02.021>.
- [15] S. Adityosulindro, C. Julcour, L. Barthe, Heterogeneous Fenton oxidation using Fe-ZSM5 catalyst for removal of ibuprofen in wastewater, *J. Environ. Chem. Eng.* 6 (2018) 5920–5928, <https://doi.org/10.1016/j.jece.2018.09.007>.
- [16] R.W. Baker, *Membranes and modules*, Membr. Technol. Appl. John Wiley & Sons, Ltd, 2004, pp. 89–160, <https://doi.org/10.1002/0470020393.ch3>.
- [17] Y.-Y. Zhang, C. He, V.-K. Sharma, X.-Z. Li, S.-H. Tian, Y. Xiong, A new reactor coupling heterogeneous Fenton-like catalytic oxidation with membrane separation for degradation of organic pollutants, *J. Chem. Technol. Biotechnol.* 86 (2011) 1488–1494, <https://doi.org/10.1002/jctb.2656>.
- [18] G. Zhang, J. Zhang, L. Wang, Q. Meng, J. Wang, Fouling mechanism of low-pressure hollow fibre membranes used in separating nanosized photocatalysts, *J. Membr. Sci.* 389 (2012) 532–543, <https://doi.org/10.1016/j.memsci.2011.11.027>.
- [19] Y. Zhang, Y. Xiong, Y. Tang, Y. Wang, Degradation of organic pollutants by an integrated photo-Fenton-like catalysis/immersed membrane separation system, *J. Hazard. Mater.* 244–245 (2013) 758–764, <https://doi.org/10.1016/j.jhazmat.2012.11.001>.
- [20] P. Bacchin, P. Aimar, R.W. Field, Critical and sustainable fluxes: theory,

- experiments and applications, *J. Membr. Sci.* 281 (2006) 42–69, <https://doi.org/10.1016/j.memsci.2006.04.014>.
- [21] Y. Lan, K. Groenen-Serrano, C. Coetsier, C. Causserand, Fouling control using critical, threshold and limiting fluxes concepts for cross-flow NF of a complex matrix: membrane BioReactor effluent, *J. Membr. Sci.* 524 (2017) 288–298, <https://doi.org/10.1016/j.memsci.2016.11.001>.
- [22] H. Chang, H. Liang, F. Qu, B. Liu, H. Yu, X. Du, G. Li, S.A. Snyder, Hydraulic backwashing for low-pressure membranes in drinking water treatment: A review, *J. Membr. Sci.* 540 (2017) 362–380, <https://doi.org/10.1016/j.memsci.2017.06.077>.
- [23] C. Causserand, S. Rouaix, J.-P. Lafaille, P. Aimar, Ageing of polysulfone membranes in contact with bleach solution: role of radical oxidation and of some dissolved metal ions, *Chem. Eng. Process. Process Intensif.* 47 (2008) 48–56, <https://doi.org/10.1016/j.cep.2007.08.013>.
- [24] E. Gaudichet-Maurin, F. Thominette, Ageing of polysulfone ultrafiltration membranes in contact with bleach solutions, *J. Membr. Sci.* 282 (2006) 198–204, <https://doi.org/10.1016/j.memsci.2006.05.023>.
- [25] B. Pellegrin, R. Prulho, A. Rivaton, S. Thérias, J.-L. Gardette, E. Gaudichet-Maurin, C. Causserand, Multi-scale analysis of hypochlorite induced PES/PVP ultrafiltration membranes degradation, *J. Membr. Sci.* 447 (2013) 287–296, <https://doi.org/10.1016/j.memsci.2013.07.026>.
- [26] E. Neyens, J. Baeyens, A review of classic Fenton's peroxidation as an advanced oxidation technique, *J. Hazard. Mater.* 98 (2003) 33–50, [https://doi.org/10.1016/S0304-3894\(02\)00282-0](https://doi.org/10.1016/S0304-3894(02)00282-0).
- [27] S.-S. Lin, M.D. Gurol, Catalytic decomposition of hydrogen peroxide on iron oxide: kinetics, mechanism, and implications, *Environ. Sci. Technol.* 32 (1998) 1417–1423, <https://doi.org/10.1021/es970648k>.
- [28] M. Hartmann, S. Kullmann, H. Keller, Wastewater treatment with heterogeneous Fenton-type catalysts based on porous materials, *J. Mater. Chem.* 20 (2010) 9002–9017, <https://doi.org/10.1039/C0JM00577K>.
- [29] A. Azzouz, E. Ballesteros, Influence of seasonal climate differences on the pharmaceutical, hormone and personal care product removal efficiency of a drinking water treatment plant, *Chemosphere* 93 (2013) 2046–2054, <https://doi.org/10.1016/j.chemosphere.2013.07.037>.
- [30] A. Ziyilan, N.H. Ince, The occurrence and fate of anti-inflammatory and analgesic pharmaceuticals in sewage and fresh water: Treatability by conventional and non-conventional processes, *J. Hazard. Mater.* 187 (2011) 24–36, <https://doi.org/10.1016/j.jhazmat.2011.01.057>.
- [31] B. Espinasse, P. Bacchin, P. Aimar, Filtration method characterizing the reversibility of colloidal fouling layers at a membrane surface: Analysis through critical flux and osmotic pressure, *J. Colloid Interface Sci.* 320 (2008) 483–490, <https://doi.org/10.1016/j.jcis.2008.01.023>.
- [32] The kinetics of complex formation between Ti(IV) and hydrogen peroxide - O'Sullivan - 2007 - International Journal of Chemical Kinetics - Wiley Online Library, (n.d.). <https://onlinelibrary.wiley.com/doi/full/10.1002/kin.20259> (accessed May 3, 2019).
- [33] C.Y. Tang, Y.-N. Kwon, J.O. Leckie, Effect of membrane chemistry and coating layer on physicochemical properties of thin film composite polyamide RO and NF membranes: I. FTIR and XPS characterization of polyamide and coating layer chemistry, *Desalination* 242 (2009) 149–167, <https://doi.org/10.1016/j.desal.2008.04.003>.
- [34] E. Arkhangelsky, D. Kuzmenko, N.V. Gitis, M. Vinogradov, S. Kuiry, V. Gitis, Hypochlorite Cleaning Causes Degradation of Polymer Membranes, *Tribol. Lett.* 28 (2007) 109–116, <https://doi.org/10.1007/s11249-007-9253-6>.
- [35] K. Yadav, K. Morison, M.P. Staiger, Effects of hypochlorite treatment on the surface morphology and mechanical properties of polyethersulfone ultrafiltration membranes, *Polym. Degrad. Stab.* 94 (2009) 1955–1961, <https://doi.org/10.1016/j.polymdegradstab.2009.07.027>.
- [36] R. Prulho, S. Therias, A. Rivaton, J.-L. Gardette, Ageing of polyethersulfone/polyvinylpyrrolidone blends in contact with bleach water, *Polym. Degrad. Stab.* 98 (2013) 1164–1172, <https://doi.org/10.1016/j.polymdegradstab.2013.03.011>.
- [37] S. Rouaix, C. Causserand, P. Aimar, Experimental study of the effects of hypochlorite on polysulfone membrane properties, *J. Membr. Sci.* 277 (2006) 137–147, <https://doi.org/10.1016/j.memsci.2005.10.040>.